

Design and Control of a Robot for the Assessment of Psychological Factors in Prosthetic Development

P. Beckerle^{1,4}, O. Christ², J. Wojtusich³, J. Schuy¹, K. Wolff², S. Rinderknecht¹, J. Vogt², O. von Stryk^{3,4}

¹Dept. of Mechanical Engineering, ²Dept. of Human Science, ³Dept. of Computer Science, ⁴Member, IEEE

¹Inst. for Mechatronic Systems, ²Work and Engineering Psychology, ³Simulation, Systems Optimization, and Robotics
Technische Universität Darmstadt — Darmstadt, Germany

lastname@ (¹ims.tu-darmstadt.de | ²psychologie.tu-darmstadt.de | ³sim.tu-darmstadt.de)

Abstract—This paper introduces a robotic concept for the assessment of psychological factors in prosthetic design. Its aim is to imitate the postural movements of the participants while those are conducting squatting movements in order to investigate the integration of artificial limbs to the subject's body scheme. Therefore, the robot mimics the functionality and appearance of the human foot, shank and thigh as well as the ankle and knee joint. To induce a more realistic outer appearance, the hull of a shop-window mannequin is used as cladding. The robot is controlled by a computed torque control combined with a RGB-D sensor for the acquisition of the desired trajectories from the participant. In the test setup one leg of the participant is hidden from his view while the robot stands next to him and imitates the movements of this leg. This paper gives an insight in the theory of body schema integration. The concept of the robot is described and detailed information about the mechanical design and actuator dimensioning in accordance with psychological and biomechanical requirements are given. Furthermore, the concept of the human-machine interface, the control algorithm and simulations based on experimental data from a human subject are presented.

Index Terms—Psychological Factors, Body Scheme, Development Methodology, Prosthetics, Robotics.

I. INTRODUCTION

Well-being, quality of life and autonomy of people with amputation are directly influenced by the amputation [1]. At the same time such individuals face challenges in their family and social environment [2]. According to [1], the main changing processes after the amputation are changes in the body image as well as the body scheme of the amputee. In contrast to the body image, which comprises the psychological experience, the body scheme describes the representation of the characteristics of the own body in a subconscious, neurophysiological and multisensory way [3], [4]. In [1] the occurrence of these changes of the amputees' identities are categorized in three phases. The first contact with the own amputation and the experience to be a disabled person in the future represents the first phase, which is followed by the actual change of identity, body image and body scheme in the second. Subsequently in the third phase, a new identity is formed caused by the amputation. Throughout these phases several negative emotions might arise and thus social support as well as individual factors i.e., how the amputation is experienced, are supporting a positive rehabilitation process of amputees, an integration of the prosthesis to their body scheme and a positive self appearance through the new body image [1], [3],

[5], [6]. As shown in [3], [5], the time after the amputation represents another important factor for the integration of the prosthesis to the amputee's body scheme. Due to [1], [3], [5] functional limitations seem to have major influence on the well-being and quality of life of the prostheses' users. Hence, a functional adaptation to the prosthesis is successful, if both, the artificial and the intact extremity, are equally integrated and represented in the body scheme and body image [3]. Additionally, feelings of unrealistic body parts are related to deficits in human information processing and can occur as a part of phantom sensations after amputation [7]. As shown in [3], [6], amputees require up to four years for the re-regulation of such sensations. These symptoms are discussed in [4] and suggest disturbances in the experience of the body scheme and image. Further, there exists a direct link to the sense of having control over the own body. As shown in [8], the body image can experimentally be manipulated in healthy volunteers. Here, the feeling of the ownership of an artificial limb and a measurable proprioceptive re-calibration towards this was induced by synchronously brushing the hidden real hand and a visible rubber hand leading to the term Rubber Hand Illusion (RHI). This illusion seems to be caused by a multisensory integration of visual, tactile and proprioceptive information.

A first systematic overview regarding the evoked Rubber Hand Illusion during movement and its maintaining factors is given in [9] and showed that movements induce a more global and stable illusion. In this paper the authors present a robotic concept for the transfer of the RHI to the lower limb and the experimental validation of the findings summarized in the introduction in analogy to the RHI experiment in [10]. With this approach the investigation and assessment of a Rubber Leg Illusion (RLI) and its utilization for user-centered prosthetic design become achievable. Section II introduces the test design and the robotic device based on the theory of body scheme integration. Subsequently, detailed information about the mechanical design in accordance to psychological and biomechanical requirements are given in Section III. In Section IV, the concept of the planned human-machine interface (HMI) and information on the control algorithm are presented as well as first simulation results for evaluation based on experimental data. Finally, a conclusion and an outlook on the authors' future works are given in Section V.

II. CONCEPT

In order to investigate the effect of a Rubber Leg Illusion itself, its maintaining factors and its occurrence during movement, a number of tests are designed. Beyond the transfer of the initial experiment on the Rubber Hand Illusion from [8] to the lower limb [11], the robotic device presented in this paper aims to examine the RLI during postural movements. The influence of movements on the illusion is an important point for its establishment in the everyday life of amputees. Since the results of [12] indicated a lack of satisfaction in postural motor functioning irrespective of the prosthesis technology, the investigation of such movements seems to be a relevant issue for the deduction of user-centered parameters for prosthetic design. Further, appearance was assessed as a descriptor for subjective body scheme integration and significantly ($p < 0.001$) correlated with the satisfaction with postural movements ($r = 0.58$). Due to this and the conclusion from [12] that appearance seems to be an important factor for body scheme integration that is associated to the conditions that deal with movements, postural movements are considered in the proposed test design.

A. Fundamental Test Design

For the experimental validation of these findings regarding postural movements, a robotic approach to simulate the sagittal plane of the human leg in postural movements is designed. During the test, the participant stands close to the robot and performs a squatting task while the robot acquires and imitates the subject's movements. At the same time, the imitated leg of the participant is hidden to enable the occurrence of a RLI with the robot.

In a first group of subjects, the influence of synchronous and asynchronous feedback of the robot on the RLI is planned to be examined as the independent variable. Based on testing this, a possible increase of the illusion by synchronicity could be acquired comparable to approach presented in [13] for the RHI. Besides, it is tested as a control condition whether the illusion can be induced without any movements by the participant, if the subject only observes the movements of the robot. Within a second group, the distance to the robot is proposed as the investigated independent variable. Since the location showed to be a significant predictor of proprioceptive displacement in [14], the distance to the robot should represent an important factor to the quality of the illusion. Hence, the proprioceptive drift regarding the robot is analyzed as the dependent variable as well as the evaluation of the questionnaire from [14] in both groups. As in [15] lower temperature of the patient's hand showed to increase the strength of the RHI, this also might be taken into account for the assessment of the RLI as a control variable. Further, electrodermal activity seems to be an optional control variable to be considered in the evaluation of the RLI as shown for the RHI in [16], [17]. In all tests, the ambient temperature and the ambient sounds are recorded as control variables. Additionally, the expectations of the participants are evaluated and a control questionnaire is analyzed.

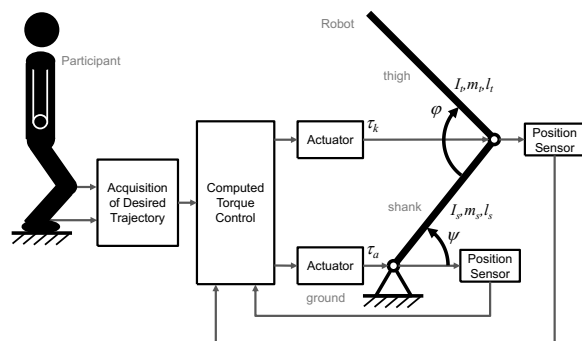


Figure 1. Block diagram of the robot's functional units

B. Robotic Concept

Figure 1 depicts a block diagram of the functional units of the robot. The mechanical design imitates foot, shank and thigh as well as the knee and ankle joint considering the appearance and functionality of these biomechanical units. During the experiments, it is placed close to the participant to support the occurrence of a RLI. Simultaneously, a motion capturing system acquires the desired trajectories from the participant's leg contactlessly. This system is connected to a real time control platform, which runs the control algorithm that operates the actuators based on the sensor data feedback acquired by measuring the movements of the robot.

III. DESIGN

Beyond, the simple robotic approach a number of psychological and biomechanical requirements have to be considered during its design in order to avoid disturbances of the Rubber Leg Illusion. Hence, a detailed description of those requirements to the robot in general as well as particular functional units are given and the design of the robot is elaborated.

A. Psychological and Biomechanical Requirements

The main requirements to the robot are to imitate the movements of the participant and to evoke a RLI. Hence, disturbances to the illusion have to be avoided and supporting factors have to be implemented in the design. As proximity supports the effect of the illusion [18], the robot has to be placed closely to the participants during the test. A distance of 0.1 – 0.2 m seems to be appropriate due to the result from [18] that the RHI was decaying significantly after a distance of 0.3 m. Further, the outer appearance of the robot is required to be as similar to the natural role model - especially in shape and laterality - as possible, since this additionally supports the occurrence of the illusion [19]. Thus, all disturbances to the natural characteristics of the human body such as visible mechanical parts - e.g., guide rails - or sounds - e.g., from actuators and gears - have to be avoided. In order to customize the outer appearance of the robot to the body geometry of the particular participant, the thigh and shank segment have to be adjustable in length. This adjustment demands a range of 0.339 – 0.457 m for the shank segment and 0.294 – 0.410 m for the thigh segment, since these are

the ranges in the body dimensions of the 5th percentile female (minimum peer group) and the 95th percentile male people (maximum peer group) [20]. Here, the length of the shank is supposed to be the distance between the ankle and the knee joint, while the length of the thigh is considered to be the distance between the height of the basis sedens and the height of the knee joint. Another requirement to the final systems is a transportable solution, since it might be necessary to visit participants for the conduction of the experiments.

Considering the mechanics of the robot, the cladding is required to deliver an intact and natural image of the human leg. The supporting structural elements inside this hull should be designed in leighthweight construction to minimize actuation effort and hence acoutstic disturbances. For the design of joints, the solution for the knee is required to provide angles up to 180° as derived in [21]. Although only angles of up to about 40° were measured during squats in [22], the ankle joint is required to provide up to 90° to compensate the negelected kinematic influence of the toe joints in the proposed design. Although the biomechanical functionality of the knee joint does not correspond to a simple one-axis joint, this should not affect its visual appearance and hence the RLI negatively. Due to this and the limitation to the sagittal plane, the simplification to implement all joints with a single axis should be valid. Furthermore, the dimensions of the shop-window mannequin limit the installation spaces to about 0.085 m for the knee joint and 0.050 m for the ankle joint.

According to the requirements, a minimalistic dimensioning of the actuators is required to minimize acoustic disturbances. Further, actuators with lower power have the advantage to be smaller and hence less conspicuous. For dimensioning of the power of the actuators, the time required to perform a squat is essential. In case of the squat-to-reach task from the standing position this time was determined to be 2.49 ± 0.55 s in younger adults [23]. In [21] the time of fast squat is considered to last 2 s distributed equally between descent and ascent. Regarding the sensors, the main focus lies on the motion capturing system, which is required to work contactless in order to not disturb the illusion. Additionally, the sensors measuring the joint angles of the robot have to be selected to be inconspicuous as possible. According to the findings in [24], the delay between the movements of the participant and the robot has to be less than 0.1 s. Additonally, this requirement is supported by the results of [25] showing that a stronger RHI effect occurs for delays below 0.3 s. Thus, the computation time that is necessary from acquiring the sensor data to sending control signals to the drives is limited to this value. As the fundamental mechanical system behind this robot is a double inverse pendulum in Up-Up position [26] and hence a instable system, a controller is required to stabilize it.

B. Mechanical Design

The hull of a shop-window mannequin is used as a cladding for the mechanical parts of the robot, since it represents an appropriate solution to provide a natural image. In order to allow the squatting movements, the thigh, shank and foot

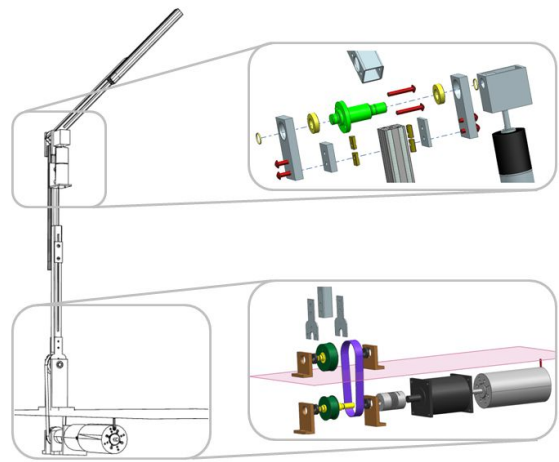


Figure 2. Mechanical design of the robot

segments of the cladding are detached at the knee and the ankle joint. Additionally, material in the movement space is removed for that purpose. Figure 2 depicts the mechanical design of the overall system without the shop-window mannequin cladding and detailed exploded vies of the joints. According to the requirements and the limited installation space in the cladding, a compact and leighthweight construction consisting of aluminium profiles is chosen for the structural elements. As a simple solution to adjust the lengths of the links of the robot, two profiles, that are relocatable to each other via a sliding carriage, are used. Due to the position of the knee actuator, the shank segment provides a range of 0.340 – 0.480 m for the adjustment. Hence, it might not be possible to adjust this value to the very smallest participants. Regarding the thigh segment, the length adjustment provides 0.252 – 0.461 m and should suit all participants. Thus, the majority of the possible test population is covered, since the 5th percentile female and the 95th percentile male people represent an appropriate group.

Knee and ankle joint are implemented as simple one-axis joints providing the required angular ranges. The detailed exploded view presented in figure 2 shows the one-axis setup of the knee joint. As shown in this figure, the actuator is directly attached to the upper shank profile and connected to the knee shaft by a gearbox. In order to keep the available installation space of 0.085 m, the dimensions of this gearbox is limited to 0.4 m considering a profile width of 0.2 m and reserve space. This design leads to a compact solution and minimizes the inertia of the thigh segment. Due to this, the knee actuator can be dimensioned smaller and the intertia of the overall system is reduced leading to lower requirements to the actuator of the ankle joint.

For an additional reduction of the intertia of the whole system, the actuator driving the ankle joint is installed in the ground structure below the participant as shown in figure 2. This also allows to shield the participants against optical and acoustic influences of this actuator. Beyond this, placing this actuator below the foot is beneficial, since the shop-window mannequin provides very limited installation space in this area.

For the transmission of the torque from the actuator to the shaft in the ankle joint, a toothed belt drive is used, since this should be more quiet than a chain drive and more compact than a solution consisting of gear wheels.

C. Dimensioning of Actuators and Transmissions

To achieve a transportable solution for the overall system, electric drives are determined as the best solution, since those actuators can be operated with the electrical net in almost every room. With Lagrange equations of the second kind [27], the dynamic equations of the system can be determined as

$$\tau = M(q)\ddot{q} + C(\dot{q}, q) + G(q). \quad (1)$$

In this, $M(q) = [m_{11} \ m_{12}; m_{21} \ m_{22}]$ contains the elements given in table I and $C(\dot{q}, q)$ and $G(q)$ are specified as

$$C(\dot{q}, q) = \begin{bmatrix} 2m_t l_s l_{t'} \sin(\varphi) \dot{\psi} \dot{\varphi} - m_t l_s l_{t'} \sin(\varphi) \dot{\varphi}^2 \\ -m_t l_s l_{t'} \sin(\varphi) \dot{\psi}^2 \end{bmatrix},$$

$$G(q) = \begin{bmatrix} g((m_s l_s + m_t l_s) \cos(\psi) - m_t l_{t'} \cos(\psi - \varphi)) \\ m_t g l_{t'} \cos(\psi - \varphi) \end{bmatrix}.$$

In the dynamic equations $q = [\psi \ \varphi]^T$ represents the vector of angular positions and $\tau = [\tau_a \ \tau_k]^T$ the torque vector. The reduced inertia I_a regarding the ankle joint is considered according to [27]. These equations are evaluated in a numerical dynamics simulation with the parameters given in Table II. As mentioned above, 2 s are assumed to be the duration of a fast squat. Hence, for ensuring a reliable operation in extreme situations, a duration of 1.5 s per squat is considered for the dimensioning of the drives. Sinusoidal trajectories, that are comparable to the biomechanical ones, are used as desired trajectories in this evaluation: $30^\circ - 180^\circ$ for the knee joint and $30^\circ - 90^\circ$ for the ankle joint. This leads to the requirements of an angular velocity of $\dot{\varphi} = 3.49 \frac{\text{rad}}{\text{s}}$ at the knee joint and $\dot{\psi} = 1.40 \frac{\text{rad}}{\text{s}}$ at the ankle joint. The results of the simulation are presented in Figure 3. With this, a maximum required torque of $\tau_{k,req} = 1.32 \text{ Nm}$ is determined for the knee actuator. The actuator of the ankle joint is required to provide a maximum torque of $\tau_{a,req} = 9.49 \text{ Nm}$. The lower plot in Figure 3 depicts the power requirements in this simulation, showing a demand of $P_{k,req} = 4.16 \text{ W}$ for the knee actuator and $P_{a,req} = 13.78 \text{ W}$ for the ankle actuator. Based on these values, a Bühler DC gear motor 1.61.077.415 is selected for the knee actuator, while a Bühler DC motor 1.13.063.407 is chosen to drive the ankle joint. With its internal gear ratio of 1 : 135 and a power of 4.34 W, the knee actuator is able to provide the required angular velocity in combination with the

Table I
ELEMENTS OF THE MASS MATRIX

Elem.	Content
m_{11}	$m_s l_s^2 + m_t l_s^2 - 2m_t l_s l_{t'} \cos(\varphi) + m_t l_{t'}^2 + I_a + I_{t,r}$
m_{12}	$-(m_t l_s l_{t'} \cos(\varphi) + m_t l_{t'}^2 + I_{t,r})$
m_{21}	$m_t l_s l_{t'} \cos(\varphi) - m_t l_{t'}^2 - I_{t,r}$
m_{22}	$m_t l_{t'}^2 + I_{t,r} + I_{t,m}$

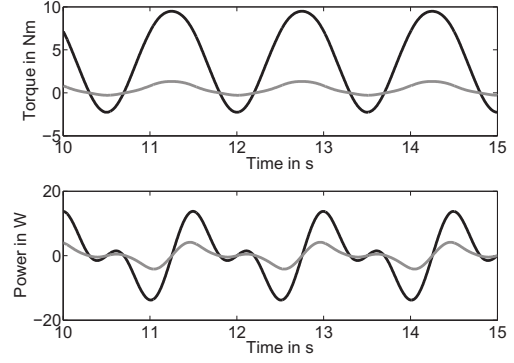


Figure 3. Simulation - Top: output torque, Bottom: motor power (solid black lines: ankle joint, solid grey lines: knee joint)

required torque in nearly all cases. Yet, the motor has to be operated with a higher voltage of below 18.00 V to reach the required angular velocities in every situation, as its rotational speed scales linearly with voltage due to the manufacturer. This is appropriate, since such high values only appear temporary in the zero-crossings and electric drives show good overload capability. A possible reduction of the lifetime of the motor is assessed to be unncritical, since the scenario described above marks the maximum requirement in the rarely emerging case that a participant exhausts the limits of the system. Anyhow, the motors inertia is kept low by this selection, leading to a more compact design and decreased requirements to the ankle actuator. As the ankle actuator delivers a torque of $\tau_{a,max} = 0.4 \text{ Nm}$ at an angular velocity $\dot{\psi}_{max} = 356.05 \frac{\text{rad}}{\text{s}}$ in its nominal range, a gear ratio of 1 : 50 is determined to provide an output torque of up to $\tau_{a,max} = 20.00 \text{ Nm}$ at a sufficient angular velocity. As both actuators are equipped with optical two-channel encoders, those are used as a compact sensor solution for the measurement of the joint angles.

Table II
PARAMETERS OF MECHANICAL SETUP AND CONTROL

	Parameter	Value	Unit	Description
mechanics	I_a	0.291	kgm^2	reduced ankle inertia
	$I_{t,r}$	0.030	kgm^2	thigh profile inertia
	$I_{t,m}$	0.029	kgm^2	knee actuator inertia
	m_s	1.788	kg	shank mass
	m_t	0.288	kg	thigh mass
	l_s	0.600	m	shank length
	l_t	0.600	m	thigh length
	$l_{s'}$	0.500	m	dist. COM(shank)-ankle
	$l_{t'}$	0.300	m	dist. COM(thigh)-knee
	g	9.81	$\frac{\text{m}}{\text{s}^2}$	gravity
control	$k_{p,a}$	800	Nm rad^{-1}	proportional gain, ankle
	$k_{v,a}$	30	Nm s rad^{-1}	derivative gain, ankle
	$k_{p,k}$	400	Nm rad^{-1}	proportional gain, knee
	$k_{v,k}$	17	Nm s rad^{-1}	derivative gain, knee

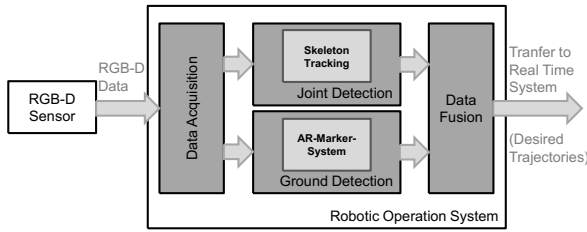


Figure 4. Desired Trajectory Acquisition Concept

IV. HUMAN-MACHINE INTERFACE AND CONTROL

A contactless acquisition of the desired trajectories for the control algorithm is required to avoid disturbances of the Rubber Leg Illusion. Thus, a concept for a possible implementation for such a motion tracking system based on a RGB-D sensor is described subsequently. Further, the computed torque control based on these trajectories is described. In order to evaluate the control algorithm under realistic circumstances without the real robot and human-machine interface, simulations assuming model deviations and using measured data from experiments with human subjects instead of the trajectories to be acquired from the motion tracking system are performed.

A. Concept for the Human-Machine Interface

As the motion tracking system provides the desired trajectories for the control, it represents the interface between the participant and the robot in this scenario. In this concept the RGB-D sensor is used to track the joint angles by utilizing skeleton tracking of the lower limbs to determine the positions of hip, knee and ankle of both legs. With this data the knee angle can easily be determined with the positions of shank and thigh. One possibility to realize such a setup is to integrate the Microsoft Kinect™ camera with the Robot Operating System (ROS) via OpenNI and the NITE package for the determination of the joint positions [28]. As it is not possible to track the ankle angle with the OpenNI package and PrimeSense NITE middleware [28], [29], additional information has to be integrated. For that purpose, the estimation of the ground surface with an AR-marker system might be an appropriate solution allowing to calculate the angle between shank and ground. To implement this motion tracking system running under ROS on the real time platform controlling the drives, Orocos can be used in combination with a real time Linux kernel such as the real time Preemption-Patch [30], [31].

B. Control Design

For the stabilization of the robot, a computed torque control is used. It combines a feedforward and feedback control in a nonlinear control law leading to a linearized closed-loop system by compensating inertia and gravity effects [32]. This is realized by an analytical inverse dynamics model of the system based on its dynamic equations for the feedforward control and an iteratively tuned PD feedback controller. With (1), the control law can be determined as

$$\tau = M(q) [\ddot{q}_d + k_p \dot{\tilde{q}} + k_v \tilde{q}] + C(\dot{q}, q) + G(q) \quad (2)$$

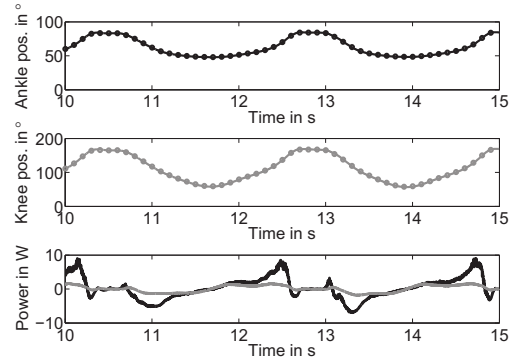


Figure 5. Simulation with experimental desired trajectories and model deviations - *Top*: angular position of ankle, *Middle*: angular position of knee, *Bottom*: motor power (black: ankle joint, grey: knee joint, solid line: real trajectories, circle: desired trajectories)

where the matrices $M(q)$, $C(\dot{q}, q)$ and $G(q)$ are according to the ones given in (1). Further, the diagonal matrices $k_p = \text{diag}(k_{p,a} \ k_{p,k})$ as well as $k_v = \text{diag}(k_{v,a} \ k_{v,k})$ contain the control parameters given in Table II while the vector $\tilde{q} = q_d - q$ represents the control error of the system.

C. Simulation with Experimental Trajectories

Since the HMI of the robot is not implemented up to this point, the feasibility of the control algorithm is evaluated based on experimental data provided by the Locomotion Laboratory at Technische Universität Darmstadt. With the trajectories of the marker positions in this experimental measurements, the trajectories of the angular position of ankle and knee joint in a squatting task are determined and used as desired trajectories. During the experiment, the participant is burdened with an additional load of 60 kg and performs seven squatting movements with a mean duration of approximately 2.30 s per squat. Beyond this, model deviations in the computed torque control are considered to test the robustness of the algorithm. Hence, all mass and inertia parameters of the system are set to 75% of their real value for the control design.

The resulting desired trajectories are given by the black circles in the top and the grey circles in middle plot of Figure 5. As depicted in the upper two plots, the control is able to track the desired trajectories even with deviating model parameters. The bottom plot of Figure 5 shows the required motor power in the experiment. These requirements are 8.98 W for the ankle motor and 1.85 W for the knee motor. Due to the lower cycle time, the load situation of the drives is decreasing and the power of both actuators is sufficient without overloading.

V. CONCLUSION

Based on the theoretic background of the Rubber Hand Illusion, this paper proposes a robot to investigate a Rubber Leg Illusion. Section II presents the concept of the robot, which is imitating a human leg in a squatting task. With the proposed test design, it is used to investigate the maintaining factors of the RLI and its occurrence during movement aiming

on the deduction of user-centered parameters for prosthetic design. The synchronicity of the stimulation and the distance between human and robot are determined to be the independent variables. Additionally, proprioceptive drift, influence of temperature and the electrodermal activity are identified to be important factors and thus be considered. To avoid disturbances of the RLI by the robot itself, such factors are identified and considered in its design. Thus, the mechanical design and the dimensioning of actuators and transmissions are based on previously elaborated psychological and biomechanical requirements. The optimization of the robot to those factors is accompanied by some issues in its implementation, which are also discussed in Section III. In Section IV a concept for the human-machine interface based and the applied computed torque control are described. To test the control algorithm and the drive train under more realistic circumstances, a simulation based on experimental data from a human subject and a deviating model is performed. The results show that the system is stabilized, the drives operate in their specifications mostly and good trajectory tracking can be achieved.

In their future work the authors will finalize the design of the psychological experiments. Among the technical issues, the implementation of the HMI based on the RGB-D sensor and the control algorithm will be addressed. This will include interface issues as well as the practical realization of the controller. Subsequently, the robot will be implemented in hardware, the control system and drive train will be optimized and the psychological experiments will be deducted. Beyond this, the authors work on a novel prosthetic simulator to enable the assessment of prostheses in pre-prototype status and to improve and complement user-centered design based on surveys and experiments with amputees [33].

ACKNOWLEDGMENT

The authors thank M. Schaarschmidt and A. Seyfarth from the Locomotion Laboratory at Technische Universität Darmstadt for providing experimental data. Further, the authors thank Bühler Motor GmbH for design support and motor sponsoring. This work was funded by Forum for Interdisciplinary Research of Technische Universität Darmstadt.

REFERENCES

- [1] H. Senra, R. Aragao Oliveira, I. Leal, and C. Vieira, "Beyond the body image: a qualitative study on how adults experience lower limb amputation," *Clinical Rehabilitation*, vol. 26, pp. 180–191, 2011.
- [2] J. Unwin, L. Kacperk, and C. Clarke, "A prospective study of positive adjustment to lower limb amputation," *Clinical Rehabilitation*, vol. 23, pp. 1044–1050, 2009.
- [3] A. Mayer, K. Kudar, K. Bretz, and J. Tihanyi, "Body schema and body awareness of amputees," *Prosthetics and Orthotics International*, vol. 32(3), pp. 363–82, 2008.
- [4] S. Gallagher and J. Cole, "Body Schema and Body Image in a Deaf-ferented Subject," *Journal of Mind and Behavior*, vol. 16, pp. 369–390, 1995.
- [5] O. Horgan and M. MacLachlan, "Psychosocial adjustment to lower-limb amputation: A review," *Disability and Rehabilitation*, vol. 26, pp. 837–850, 2004.
- [6] C. Murray and J. Fox, "Body image and prosthesis satisfaction in the lower limb amputee," *Disability and rehabilitation*, vol. 24 (17), pp. 925–931, 2002.
- [7] A. I. Goller, K. Richards, S. Novak, and J. Ward, "Mirror-touch Synaesthesia in the Phantom Limbs of Amputees," *Cortex*, vol. <http://dx.doi.org/10.1016/j.cortex.2011.05.002>, 2012.
- [8] M. Botvinick and J. Cohen, "Rubber hands 'feel' touch that eyes see," *Nature*, vol. 391, p. 756, 1998.
- [9] O. Christ, M. Jokisch, J. Preller, P. Beckerle, S. Rinderknecht, and J. Vogt, "Persistence of the rubber hand illusion and maintaining factors during active or passive movements: new indicators for rehabilitation?" *European Psychiatry*, vol. 27 (S1), p. 224, 2012.
- [10] B. Rosen, H. H. Ehrsson, C. Antfolk, C. Cipriani, F. Sebelius, and G. Lundborg, "Referral of sensation to an advanced humanoid robotic hand prosthesis," *Scandinavian Journal of Plastic and Reconstructive Surgery and Hand Surgery*, vol. 43, pp. 260–266, 2009.
- [11] M. Jokisch, J. Preller, A. Schropp, C. Christ, P. Beckerle, and J. Vogt, "The rubber hand illusion paradigm transferred to the lower limb: A physiological, behavioral and subjective approach," *16th world congress of psychophysiology (submitted)*, 2012.
- [12] O. Christ, P. Beckerle, S. Rinderknecht, and J. Vogt, "Usability, satisfaction and appearance while using lower limb prostheses: Implications for the future," *Neuroscience Letters*, vol. 500 (S1), p. e50, 2011.
- [13] E. Lewis and D. M. Lloyd, "Embodied experience: A first-person investigation of the rubber hand illusion," *Phenomenology and the Cognitive Sciences*, vol. 9, pp. 317–339, 2010.
- [14] M. R. Longo and P. Haggard, "Sense of agency primes manual motor responses," *Perception*, vol. 38, pp. 69–78, 2009.
- [15] M. P. M. Kammers, K. Rose, and P. Haggard, "Feeling numb: Temperature, but not thermal pain, modulates feeling of body ownership," *Neuropsychologia*, vol. 49, pp. 1316–1321, 2011.
- [16] K. C. Armel and V. S. Ramachandran, "Projecting sensations to external objects: evidence from skin conductance response," *Proceedings of the Royal Society, B, Biological Sciences*, vol. 270, pp. 1499–1506, 2003.
- [17] M. Slater, D. Perez-Marcos, H. H. Ehrsson, and M. V. Sanchez-Vives, "Inducing illusory ownership of a virtual body," *Frontiers in Neuroscience*, vol. 3 (2), pp. 214–220, 2009.
- [18] D. M. Lloyd, "Spatial limits on referred touch to an alien limb may reflect boundaries of visuo-tactile peripersonal space surrounding the hand," *Brain and Cognition*, vol. 64, pp. 104–109, 2007.
- [19] M. Tsakiris, M. R. Longo, and P. Haggard, "Having a body versus moving your body: Neural signatures of agency and body-ownership," *Neuropsychologia*, vol. 48, pp. 2740–2749, 2010.
- [20] H. Greil, "Körpermaße 2000: Aktuelle Perzentilwerte der deutschen Bevölkerung im jungen Erwachsenenalter," *Brandenburgische Umwelt Berichte*, 2001.
- [21] R. F. Escamilla, "Knee biomechanics of the dynamic squat exercise," *Medicine & Science in Sports & Exercise*, vol. 33, pp. 127–141, 2001.
- [22] S. Hwang, Y. Kim, and Y. Kim, "Lower extremity joint kinetics and lumbar curvature during squat and stoop lifting," *BMC Musculoskeletal Disorders*, vol. 10:15, pp. 1–10, 2009.
- [23] F.-C. Kuo, W.-P. Kao, H.-I. Chen, and C.-Z. Hong, "Squat-to-reach task in older and young adults: Kinematic and electromyographic analyses," *Gait & Posture*, vol. 33, pp. 124–129, 2011.
- [24] O. Christ, C. Weber, I. Borchert, and H. Sorgatz, "Dissonance between visual and proprioceptive information as a moderator in experimental pain," *Journal of Rehabilitation Medicine*, vol. 43(9), p. 836, 2011.
- [25] S. Shimada, K. Fukuda, and K. Hiraki, "Rubber hand illusion under delayed visual feedback," *PLoS ONE*, vol. 4(7), p. e6185, 2009.
- [26] M. Yamakita, M. Iwashiro, Y. Sugahara, and K. Furuta, "Robust Swing Up Control of Double Pendulum," *Proceedings of the American Control Conference*, vol. June, pp. 290–295, 1995.
- [27] D. Gross, W. Hauger, J. Schröder, and W. A. Wall, *Technische Mechanik 3: Kinetik*. Springer, 2010.
- [28] "ROS Wiki," 2012. [Online]. Available: <http://www.ros.org/wiki>
- [29] "PrimeSense," 2012. [Online]. Available: <http://www.primesense.com/>
- [30] "The Orocos Project," 2012. [Online]. Available: <http://www.orocos.org/>
- [31] J. Mitschang, "Harte Echtzeit unter Linux Fallstudie RTAI vs. RT-Preempt," *IESE-Report*, vol. 058.07/D, 2007.
- [32] R. Kelly, V. Santibáñez Davila, and J. A. Loría Perez, *Control of Robot Manipulators in Joint Space*. Springer, 2005.
- [33] O. Christ, J. Wojtusich, P. Beckerle, K. Wolff, J. Vogt, O. von Stryk, and S. Rinderknecht, "Prosthesis-User-in-the-Loop: User-Centered Design Parameters and Visual Simulation," *34th Annual International Conference of the IEEE EMBS (accepted)*, 2012.